

Character of Atomic Vibrations in a Lennard-Jones Glass

Philip B. Allen

Department of Physics and Astronomy, State University of New York, Stony Brook, New York 11794-3800

W. G. Harper

Department of Applied Mathematics, State University of New York, Stony Brook, New York 11794-3600

L. Angelani

INFN, SM-C-INFN, and Dipartimento di Fisica, Università di Roma La Sapienza, P.le A. Moro 2, 00185 Roma, Italy

Lennard-Jones glasses (made on a computer by quenching from liquid state coordinates) are studied in harmonic approximation. Vibrational eigenfrequencies and eigenvectors are found by exact diagonalization for models with periodic boundaries and $N = (500, 2048, \text{ and } 6980)$ atoms. We analyze the density of states, mobility edge, and bond-stretching character of the normal modes. In agreement with older work of Grest, Nagel, and Rahman, the upper 7% of the modes are localized, and the rest, delocalized. The modes can not be differentiated by any property or quantum number except their eigenfrequency. More specially, in a given narrow frequency interval, all modes are globally identical. Transverse or longitudinal character, for example, disappears.

61.43Dg, 63.50.+x, 66.70.+f

I. INTRODUCTION

Vibrational properties of disordered media have been reviewed by various authors [1-4]. Subsequent to most of these reviews, Grest, Nagel, and Rahman (GNR) [5-10] did a careful characterization of the normal modes of the Lennard-Jones (LJ) glass. Our previous numerical studies, motivated by heat conductivity experiments and by theoretical controversy, focussed on vibrations in amorphous Si (Am-Si) [11]. Here we present results for a very large LJ glass model, with local atomic structure very different from Am-Si. These results confirm the GNR picture. We use the term "glass" simply to mean an amorphous solid, and the abbreviation am-LJ to denote the LJ glass.

The model studied is a monatomic 6-12 Lennard-Jones system, $V(r) = 4[(\sigma/r)^{12} - (\sigma/r)^6]$, with potential parameters suitable for Argon: $\epsilon/k_B = 125.2 \text{ K}$ and $\sigma = 0.3405 \text{ nm}$. This potential gives a satisfactory description of crystalline Ar [12]. In its face-centered cubic (fcc) structure, each atom is surrounded by 12 nearest neighbors located a little inside the minimum of the $V(r)$ at

$r = 2^{1/6} \sigma$. The second shell is more distant by $2^{1/2} \sigma$.

Standard molecular dynamics simulations were done on systems with $N = 500, 2048$ and 6980 atoms, enclosed in a cubic box with periodic boundary conditions. A truncated ($r_c = 2.6 \sigma$) LJ potential was used. The simulated density was $\rho = 42 \times 10^3 \text{ mol/cm}^3$, corresponding to the reduced value $\rho^* = 0.85$. After an equilibration run at $T = 400 \text{ K}$ using NVE molecular dynamics, gradual cooling was performed down to a temperature ($T = 150 \text{ K}$) slightly above the melting temperature. Finally, conjugate gradient minimization found the glassy minimum configuration.

The resulting structure of am-LJ is somewhat like that of a smeared-out argon crystal. The density is about 5% smaller. There may be icosahedral aspects in the local packing [13], but our models are more similar to the "LJ glass" of Simdyankin et al. [14] than to their "IC glass" with strongly icosahedral features. A shell of radius r contains on average $(4\pi/3)r^3 \rho^*$ atoms, where ρ^* is the number density. The mean distance from an atom to its N th neighbor is thus $(3N/4\pi\rho^*)^{1/3}$.

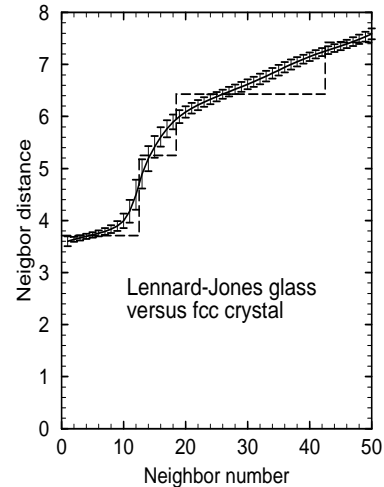


FIG. 1. mean distance to the N th neighbor, for am-LJ (solid curve) and the corresponding crystal (dashed lines). Error bars give the variance $\langle r^2 \rangle^{1/2}$ in the distribution of N th neighbor positions.

For am-LJ we calculated the mean distance to the N^{th} neighbor, and the variance $\langle r^2 \rangle^{1/2}$ of this quantity, which are plotted in Fig. (1). The closest 10 neighbors cluster in a narrow interval near the distance 3.7Å found in crystalline Ar. The 11th to 13th neighbors have less well-defined positions. The 15th to 18th atoms have the least well-defined positions, lying near the second neighbor shell of the crystal. More distant neighbors start to be packed as in a random gas, with distance starting to scale like $N^{1/3}$.

Normal modes of vibration were calculated in harmonic approximation, using the same periodic boundary conditions used to compute the positions. The calculations were done on Njal, a Beowulf cluster with 81 dualpentium III processors running at 0.933 GHz. The Scalapack routine PDSYEV was used. The largest system size, 6,980 atoms, corresponds to a real-symmetric dynamical matrix of dimension 20,940, the largest that fits conveniently into Njal's memory. This matrix required about 100 minutes to diagonalize. The vibrational density of states is shown in Fig. (2). All three models give essentially the same result, which is shown here for the 6980-atom model, and was first found by Rahman et al. [15]. The results for the glass are compared with the density of states of the crystal, which closely resembles experiment on crystalline Ar [16]. However, the LJ glass has a surprisingly different density of states, being featureless, with no distinction between longitudinal and transverse modes.

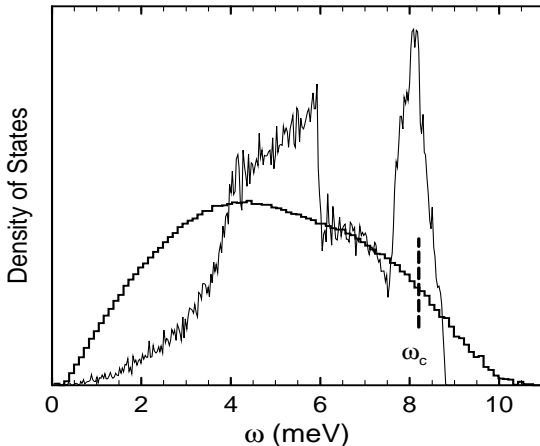


FIG. 2. Density of vibrational eigenstates of am-LJ and the corresponding fcc Lennard-Jones (argon-like) crystal. The dashed vertical line indicates the position of the mobility edge in am-LJ.

To pursue this issue, it is interesting to look at the "bond-stretching parameter" S_a of the a^{th} normal mode, defined as [17]

$$S_a = \frac{\sum_{i,j} \hat{n}_{ij} \cdot \frac{j(u_i^a - u_j^a)}{|\hat{n}_{ij}|}}{\sum_{i,j} \frac{j(u_i^a - u_j^a)^2}{|\hat{n}_{ij}|}} \quad (1)$$

where u_i^a is the displacement eigenvector on the atom with position label i and position R_i . The unit vector \hat{n}_{ij} points in the direction $R_i - R_j$. In other words, S_a measures for mode a the relative amount of stretching of each near-neighbor bond. For the crystal, this is rigorously defined by using the 12 bonds from each atom to its first neighbors. For the glass, we sum all neighbors whose separation is less than the mean distance to the 12.5th neighbor. The results are plotted in Fig. (3).

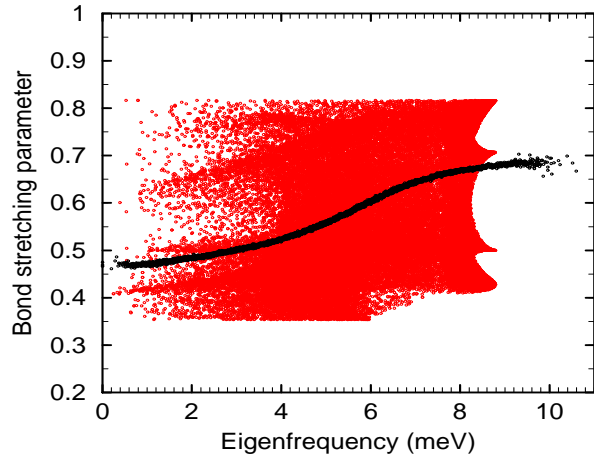


FIG. 3. Bond-stretching character versus frequency for the normal modes of the glass (narrow dark band) compared with the bond-stretching character of the normal modes of the crystal (broad light band).

This figure shows a very striking difference between the crystal and the glass. Crystalline normal modes can be labelled by the wavevector \mathbf{k} . In Ar, there are only three normal modes at each \mathbf{k} . They have usually quite different bond-stretching characters, and can normally be classified as longitudinal (L) or transverse (T). This leads to a highly differentiated spectrum of states, seen in the figure as a broad range of values of S_a at each frequency. In the glass, the bond-stretching character S_a collapses to a narrow interval whose width diminishes to zero as N increases to infinity. Lacking the quantum number \mathbf{k} , each mode has totally mixed character. This property was noticed previously for other glasses [18,19,11]. In an infinite glass, with infinitely many modes at each frequency, one could make a unitary rotation (within the subspace of fixed frequency) to a basis where certain modes would look approximately pure L in some local region. However, at long enough distances this character is completely lost. At low frequencies, purified modes defined this way could be chosen have

a fairly sharply defined local value of k . At large enough distances, the mode would evolve into a spherical mixture of different directions of k . As frequency increases, there is a crossover (the "Loe-Regel" (IR) crossover) to the regime where the local k can hardly be defined because it decays in a distance of one or two neighbors. The IR crossover and other low-frequency properties will be the subject of a future study.

It was noticed by GNR that a given normal mode, insofar as it was L, expressed its L character at specific wavevectors, and insofar as it was T, expressed that character at other wavevectors. This enabled them to draw pseudo-dispersion curves showing very different character for L and T aspects. This does not contradict our view that a given mode cannot be classified. Each mode is simultaneously L and T, probably even at the same point in space unless purified as described above.

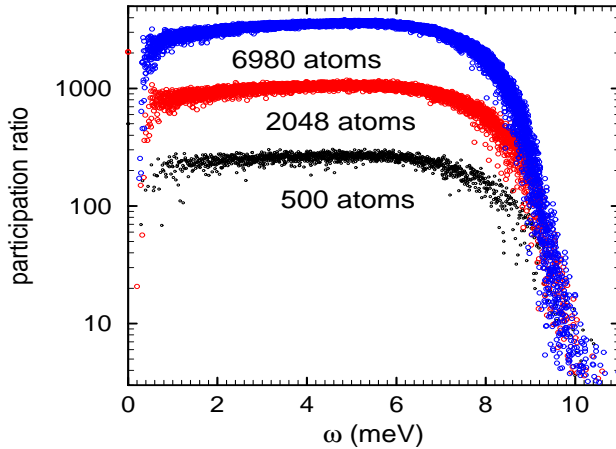


FIG. 4. Inverse participation ratio on logarithmic scale versus eigenfrequency for all normal modes of systems of various sizes.

In principle, normal modes of vibration, just like electron eigenstates in quantum theory, can be rigorously classified as extended (E) or localized (L). In three dimensions the vibrational spectrum has sharp E/L boundary frequencies ("mobility edges," ω_c) separating these two kinds of modes. The IR crossover is low in the spectrum of a glass, but the E/L boundary is usually high in the spectrum.

An hypothesis that the mobility edge coincides with the IR crossover [20] has not proved true for any model that has been studied numerically, but has remained a popular misconception. Our large system provides a useful confirmation that previous studies have correctly located the mobility edge. We compute the participation ratio p_a for each normal mode, defined as

$$p_a = \frac{\sum_i |x_i^a|^2}{\sum_i |x_i^a|^2} \quad (2)$$

The values of p_a are plotted on a logarithmic scale versus eigenfrequency for all three models in Fig. (4).

Notice first that the value of p_a hovers at slightly higher than 0.5N for a significant part of the spectrum (frequencies 2.5 to 6.5 meV). These are very well delocalized states whose amplitude does not vary too much from atom to atom. At low frequencies (below 1 meV for the 6980-atom model, and pushing up to 2 meV for the 500-atom model) there is a trend to lower values of p_a , and there occur some idiosyncratic modes with p_a reduced by 10 or more. Their interpretation remains difficult [21]. At least some of this behavior has to be attributed to finite-size artifacts. We hope to make a detailed study later. Finally, at high frequencies, very low values of p_a occur. These states are strongly Anderson localized. The mobility edge is estimated to be at $\omega_c = 8.2 \pm 0.1$ meV. This estimate was found by fitting a straight line to the logarithmic data at the point where $p_a = 0.25N$. Extrapolating this line back to the horizontal line $p_a = 0.5N$, the intersection occurs at around 8.2 meV, with uncertainty which diminishes as the system size increases. This value of ω_c corresponds to having the lower 93% of the spectrum delocalized, and the upper 7% localized, and agrees with the result of GNR [5,10].

These results make an interesting comparison to our earlier work on amorphous Si [11]. One major difference is that the density of vibrational states in am-Si retains much of the structure seen in the crystal, with acoustic and optical types of vibrations separated by a region of low density of states. To the contrary, in am-LJ, the density of states loses differentiation and is completely featureless. Apart from this, other properties of am-LJ vibrations are reminiscent of those in am-Si. We see similar behavior in the collapse of the bond-stretching character onto a single frequency-dependent curve. The anomalous states at very low frequency, and the strongly localized states at very high frequency, have similar character. In both glasses, fewer than 10% of the modes are localized, always at the upper end of the spectrum.

ACKNOWLEDGMENTS

We thank G. S. Grest, J. Fabian, J. L. Feldman and G. Viliani for help. Work at Stony Brook was supported by NSF grant DMR-0089492. We thank K. K. Likharev for the use of the Njal computer cluster, which was purchased using a grant from DOD's DURIP program.

-
- [1] R. J. Elliott and P. L. Leath, in *Dynamical Properties of Solids*, (eds. G. K. Horton and A. A. Maradudin), North Holland, Amsterdam, 1975; vol. 2, p. 385.
 - [2] D. W. Eeaire and P. C. Taylor, in *Dynamical Properties of Solids*, (eds. G. K. Horton and A. A. Maradudin), North Holland, Amsterdam, 1980; vol. 4, p. 1.
 - [3] W. M. Visscher and J. E. Gubernatis, in *Dynamical Properties of Solids*, (eds. G. K. Horton and A. A. Maradudin), North Holland, Amsterdam, 1980; vol. 4, p. 63.
 - [4] R. O. Pohl, in *Encyclopedia of Applied Physics*, Wiley-VCH, 1998, vol. 23, p. 223.
 - [5] S. R. Nagel, A. Rahman, and G. S. Grest, *Phys. Rev. Lett.* 47, 1665 (1981).
 - [6] G. S. Grest, S. R. Nagel, and A. Rahman, *Phys. Rev. Lett.* 49, 1271 (1982).
 - [7] G. S. Grest, S. R. Nagel, and A. Rahman, *Phys. Rev. B* 29, 5968 (1984).
 - [8] S. R. Nagel, G. S. Grest, and A. Rahman, *Phys. Rev. Lett.* 53, 368 (1984).
 - [9] S. R. Nagel, G. S. Grest, S. Feng, and L. M. Schwartz, *Phys. Rev. B* 34, 8667 (1986).
 - [10] S. R. Nagel, G. S. Grest, and A. Rahman, *Physics Today*, Oct. 1983, p. 24.
 - [11] P. B. Allen, J. L. Feldman, J. Fabian, and F. Wooten, *Phil. Mag. B* 79, 1715-32 (1999).
 - [12] C. Kittel, *Introduction to Solid State Physics*, 7th Edition, Wiley, New York, 1996.
 - [13] D. R. Nelson and F. Spaepen, *Solid State Phys.* 42, 1 (1989).
 - [14] S. I. Simdyankin, M. D. Zugutov, S. N. Taraskin, and S. R. Elliott, *Phys. Rev. B* 63, 184301 (2001).
 - [15] A. Rahman, M. J. Mandell, and J. P. McTague, *J. Chem. Phys.* 64, 1564 (1976).
 - [16] Y. Fujii, N. A. Lurie, R. Pynn, and G. Shirane, *Phys. Rev. B* 10, 3647 (1974).
 - [17] M. Marinov and N. Zotov, *Phys. Rev. B* 55, 2938 (1997).
 - [18] W. A. Kamitakahara, C. M. Soukoulis, H. R. Shanks, U. Buchenau, and G. S. Grest, *Phys. Rev. B* 36, 6539 (1987).
 - [19] J. Fabian and P. B. Allen, *Phys. Rev. Letters* 79, 1885 (1997).
 - [20] S. Alexander, *Phys. Rev. B* 40, 7953 (1989).
 - [21] J. L. Feldman, P. B. Allen, and S. R. Bickham, *Phys. Rev. B* 59, 3551 (1999).